A Wide-Band On-Wafer Noise Parameter Measurement System at 50–75 GHz

Mikko Kantanen, Manu Lahdes, Tauno Vähä-Heikkilä, *Student Member, IEEE*, and Jussi Tuovinen, *Member, IEEE*

***Abstract*—A wide-band on-wafer noise parameter measurement system at 50–75 GHz is presented. This measurement system is based on the cold-source method with a computer-controlled waveguide tuner. Calibrations and measurement methods are discussed and measured results for passive and active on-wafer devices are shown over a 50–75-GHz range. An InP high electron-mobility transistor device is used as a test item for the active device. A Monte Carlo analysis to study measurement uncertainties is also shown. The measurement system is a useful tool in the development and verification of device noise models, as well as in device characterization.**

***Index Terms*—Noise-parameter measurements, on-wafer characterization, wide-band measurements.**

I. Introduction

COMMERCIAL exploitation of millimeter waves is currently becoming a reality with increasing intent. The main driving force has been the development in manufacturing monolithic integrated circuits, which can currently be produced up to approximately 220 GHz. Examples of commercial millimeter-wave applications are automotive collision-avoidance radars, radio links, and local area networks. Scientific millimeter-wave research is mainly related to radio astronomy and cosmology. Millimeter waves are also very attractive to be used in imaging systems for surveillance and contraband detection. Funding for this kind of application is coming from military and law enforcement agencies. Many applications mentioned above rely on the use of low-noise amplifiers (LNA). It is desirable to model noise behavior properly as early as possible during the LNA design process to avoid expensive and time-consuming iterations. The noise properties of LNAs are usually calculated during the design process using noise parameters of transistors.

In contrast to the microwave region, noise parameters of transistors at millimeter waves are usually not given by the manufacturer or they have been extrapolated from measurements made in the microwave region using device dependent noise models. These models themselves are commonly developed at microwave frequencies and applying them in a millimeter-wave region is risky. Thus, on-wafer noise parameter measurements at millimeter-wave frequencies are needed to characterize devices and to develop and verify device dependent noise models.

Thus far, wide-band on-wafer noise parameter measurements have been carried out up to 40 GHz [1]. At 50–75 GHz, measurements covering part of the band and using a manual input tuner have been reported [2]–[4]. A partial report about the measurement system described here has been presented in [5]. Above 75 GHz, results on single frequency and for a passive device have been presented [6]. Wide-band measurements are necessary in order to detect systematic errors that may not be detected in measurements over a narrow frequency band, even if the measurement system seems to work properly otherwise. Using the measurement system described here, noise parameters of a chip device can be measured over the entire 50–75-GHz range in an automated manner.

Manuscript received March 5, 2002; revised November 6, 2002. This work was supported by the European Space Agency under Contract 1655/95/NL/MV.

The authors are with the Millimeter Wave Laboratory of Finland–Millilab, VTT TECHNICAL RESEARCH CENTRE OF FINLAND, Espoo, FIN-02044 VTT, Finland (e-mail: mikko.kantanen@vtt.fi).

Digital Object Identifier 10.1109/TMTT.2003.810129

II. Noise Parameters

Noise parameters are not directly measurable quantities, which are determined indirectly by measuring the noise figure of a linear two-port with different source impedances connected to the device-under-test (DUT). The noise figure of a linear two-port varies as a function of the source reflection coefficient, as given by the commonly known equation [7]

$$F = F_{\min} + 4r_n \frac{|\Gamma_S - \Gamma_{\rm opt}|^2}{\left(1 - |\Gamma_S|^2\right)|1 + \Gamma_{\rm opt}|^2} \tag{1}$$

where $F_{\min}$ is the minimum noise figure of the two-port, r_n is the normalized noise resistance, $\Gamma_{\rm opt}$ is the optimum reflection coefficient, with which the minimum noise figure is achieved, and Γ_S is a reflection coefficient of a network connected to the input of the two-port. Parameters $F_{\min}$, r_n, and $\Gamma_{\rm opt}$ are called noise parameters. Since $\Gamma_{\rm opt}$ is a complex quantity, at least four noise-figure measurements using different source reflection coefficients Γ_S have to be made in order to solve the noise parameters of the DUT. To reduce the effect of measurement errors, more than four measurements are often made and noise parameters are solved using mathematical fitting routines.

III. Measurement Setup

The schematics and photograph of the automated measurement setup built are presented in Figs. 1 and 2, respectively. The reference planes used in the calibrations are also shown. The so-called cold-source method [8], [9] was selected to be used. In the developed setup, an automated noise-figure meter is used to perform the noise-figure measurements. Since the frequency range of the noise-figure meter is 10–1500 MHz, a receiver chain consisting of an LNA, a mixer, and a millimeter-wave signal generator is used to downconvert the noise power from millimeter waves to 30 MHz. The LNA is obtained through

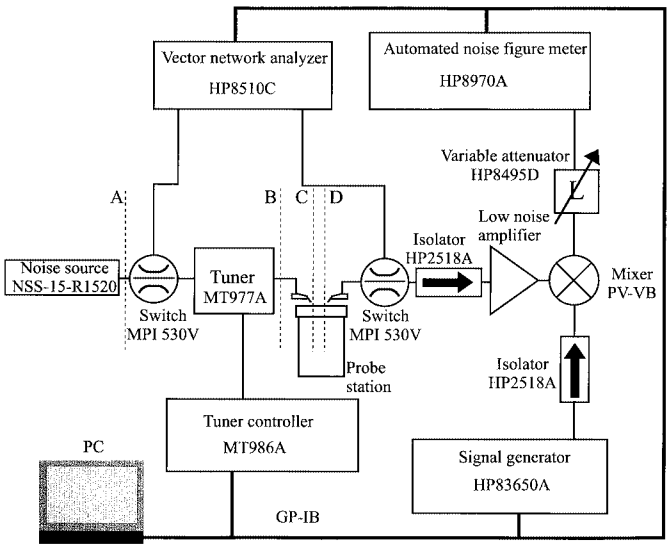

Fig. 1. Noise-parameter measurement setup.

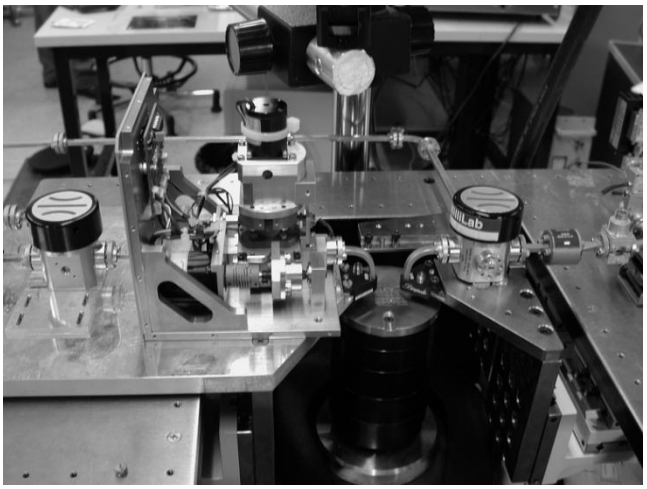

Fig. 2. Photograph of the measurement system.

Planck Surveyor collaboration [10]. A DUT is placed in a probe station and its source impedance is varied using the automated tuner. The tuner is a commercially available waveguide tuner in which the reflection coefficient at the reference plane B is controlled using a moveable probe. The magnitude of the reflection coefficient is controlled by changing probe insertion into the waveguide and the phase of the reflection coefficient is controlled moving the probe along the waveguide. The probe motions are automated by stepper motors. The probe's placement inside the waveguide can be characterized by two coordinates, which are step counts of the stepper motors. Thus, probe's placement will be referred to simply as *tuner position* below. Due to losses between the tuner and a DUT, the maximum realizable magnitude of a reflection coefficient at the DUT input is approximately 0.8. A solid-state noise source is connected to the tuner input. Bias for active devices is fed through internal bias tees of the probes. A vector network analyzer and waveguide switches are added to the measurement system in order to perform S-parameter measurements without a need of reconfiguration of the system. In-house written software is used to control measurement setup.

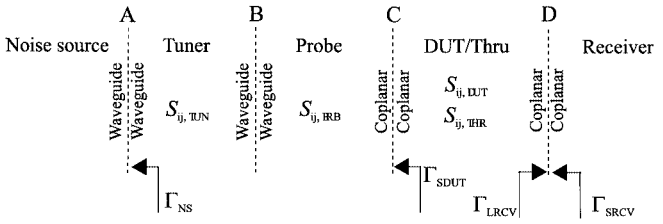

Fig. 3. Functional blocks, notations, and connection types of the measurement setup.

IV. Calibration and Measurement Procedures

From the operational point-of-view, the measurement setup can be divided into five functional blocks, which are the noise source, tuner, input probe, DUT, and noise receiver. These blocks, notation of their parameters, and connection types of the reference planes are shown in Fig. 3. The reference planes between different blocks are selected this way in order to make calibrations and calculations easier. Required measurements can be divided into three steps. The first two steps are related to the characterization of the measurement system and can be omitted if no change in the measurement system has been made. These three steps are described individually below.

A. S-Parameter and Reflection-Coefficient Measurements

In order to perform noise-parameter measurements, S-parameters of the tuner, the input probe, the DUT, and a thru calibration standard have to be known. S-parameters of one tuner position are needed in receiver calibration calculations and they are measured while the tuner probe is retracted from the waveguide and the tuner is essentially a normal waveguide. This measurement, as well as the S-parameter measurements for the DUT and the thru calibration standard, are done with a vector network analyzer in a straightforward manner. The line-reflect–reflect–match (LRRM) calibration [11] is used for the on-wafer components and waveguide thru-reflect-line (TRL) calibration [12] is used for the tuner. The calibration methods mentioned above were selected because they provided the best accuracy with existed calibration standards. Since the input probe is a noninsertable network, its S-parameters cannot be measured directly. Thus, two one-port calibrations are done, i.e., a waveguide short-offset short-load (SSL) calibration in reference plane B and a coplanar short-open-load (SOL) on-wafer calibration in reference plane C. S-parameters of the noninsertable network B–C can be calculated from the network analyzers' error correction coefficients obtained in these calibrations [13], [14].

The S-parameters of the thru standard, which are used in the calculations, are determined in the following manner. First, an LRRM calibration is done with a set of the calibration standards. S-parameters of a thru from a different set of calibration standards are then measured. These S-parameters are then used in the noise-parameter calculations. Usually, the magnitude of the S_{21} is approximately 0.99 over the entire V-band.

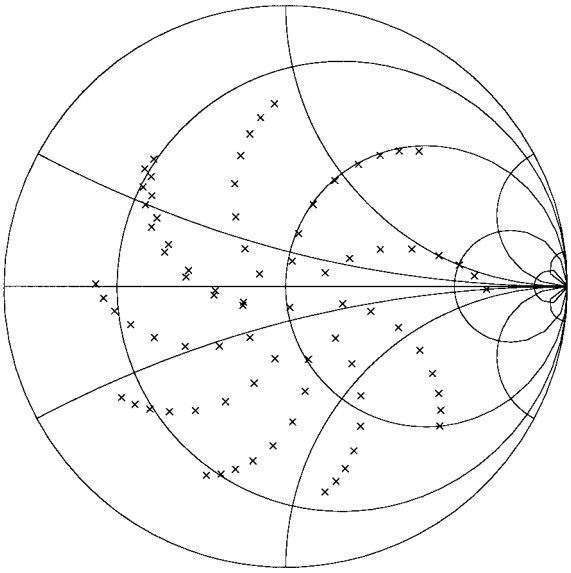

Fig. 4. Measured source reflection coefficients ($\Gamma_{S\mathrm{DUT}}$) at 57 GHz during tuner characterization.

The reflection coefficient measurements include reflection coefficients of the cold noise source (Γ_{NS}) and the receiver (Γ_{LRCV}), as well as source reflection coefficient ($\Gamma_{S\mathrm{DUT}}$) measurements with different tuner positions. The latter two operations cannot be performed directly because the port to be measured is the coplanar probe tip in both cases. Thus, the thru calibration standard is used. Instead of measuring the reflection coefficient of the receiver at reference plane D, the reflection coefficient of a cascade of the thru and the receiver is measured at reference plane C. The reflection coefficient of the receiver can then be calculated from the measured value when S-parameters of the thru are known. A similar procedure is used when source reflection coefficients at the DUT input plane are measured using different tuner positions. During these measurements, the entire input network (noise source, tuner, and input probe) is assembled and the reflection coefficient is measured for a great number of tuner positions to allow device specific selection during the later measurements. As an example, measured source reflection coefficient values at 57 GHz are shown in Fig. 4. Measurement of Γ_{NS} is a simple waveguide operation.

The accurate characterization of these passive networks is a very important issue in noise-parameter measurements. The attenuation between the noise source and receiver decreases hot noise temperature at the receiver input and inaccuracies in the source reflection-coefficient measurements directly affects the noise parameter extraction accuracy. Thus, few unidealities and assumptions in calibration methods that degrade the accuracy of passive network characterization are outlined here [15], [16]. With waveguides, the two-port TRL and one-port SSL calibrations are considered to be very accurate with manufacturer provided standard definitions. The on-wafer coplanar SOL calibration is the most sensible for standard definition errors because all calibration standards used have to be fully characterized. With LRRM calibration, only the line standard needs to be fully known, reflect standards need not to be equal, and a load inductance present in the coplanar load is calculated during the calibration. Standard definitions for SOL standards and the LRRM line were provided by the calibration substrate manufacturer and their effects are taken into account in the calibration software used for the on-wafer calibrations. The differences between the actual standard used in the calibration and the standard definitions are the main source for inaccuracies in the calibrations. These differences can occur, for example, from wearing of the standards and probes, as well as from inaccurate probe placement. Thus, there will always be residual errors in measured S-parameters.

B. Noise Receiver Calibration

To carefully characterize the noise contribution of the receiver, its kBG-factor and noise parameters have to be known. The kBG-factor is a constant on each frequency and it includes the Boltzmann's constant k, the noise bandwidth of the measurement system B, and the transducer gain G of the receiver for a 50-Ω source. During these measurements, the thru calibration standard is placed in the probe station. A more detailed description about the measurement procedure can be found in [9]. Only the most important formulas are repeated here. The kBG-factor of the receiver is determined performing one noise power measurement with a hot and a cold noise source, respectively. The kBG-factor is calculated with the following:

$$kBG = \frac{P_H - P_C}{T_H - T_C}\left|1 - \Gamma_{LRCV}\Gamma_{SRCV}\right|^2 \cdot \frac{\left|1 - S_{11,\,AD}\Gamma_{\mathrm{NS}}\right|^2}{\left(1 - \left|\Gamma_{\mathrm{NS}}\right|^2\right)\left|S_{21,\,AD}\right|^2} \quad (2)$$

where P_H and P_C are noise powers measured with a hot and a cold noise source, respectively, T_H is the noise temperature of the hot noise source calculated from the excess noise ratio (ENR) and transformed into receiver input plane, T_C is the physical temperature of the measurement system, Γ_{SRCV} is the source reflection coefficient of the input network at the receiver input reference plane (the reference plane D), Γ_{LRCV} is the reflection coefficient of the receiver, and $S_{ij,\,AD}$ are overall S-parameters of the cascaded tuner, probe, and thru.

The noise parameters of the receiver are determined by measuring noise powers of the cold noise source using at least four different tuner positions. The noise figure is obtained using

$$F_i = \frac{P_{Ci}}{T_0 kBG}\frac{\left|1 - \Gamma_{LRCV}\Gamma_{SRCVi}\right|^2}{1 - \left|\Gamma_{SRCVi}\right|^2} - \frac{T_C}{T_0} + 1 \quad (3)$$

where P_{Ci} is the measured noise power for the ith source reflection coefficient Γ_{SRCVi}, T_0 is the standard temperature 290 K, and T_C is the physical temperature of the measurement system. Using obtained noise-figure–source reflection-coefficient pairs, noise parameters are calculated using the noise parameter extraction technique described in [17] with similar modifications as suggested in [18]. In brief, exact solutions of four $F_i - \Gamma_{SRCVi}$ pair subsets are calculated at first. Errors between values calculated using this solution and measured values are then derived. After all possible four pair subsets are investigated, solutions with which the error remained within predetermined boundaries are averaged to produce the final noise parameters. In these measurements, 20% of error was allowed for each value.

C. Noise-Parameter Measurements of the DUT

After the calibrations, the DUT is placed in the probe station. During this phase, only the cold noise source is used with different tuner positions. The total noise figure of the cascade of the DUT and receiver can be calculated using

$$F_{\mathrm{TOT}i} = \frac{P_{Ci}}{T_0 kBG} \cdot \frac{|1-S_{11,\mathrm{DUT}}\Gamma_{S\mathrm{DUT}i}|^2\,|1-\Gamma_{LRCV}\Gamma_{SRCVi}|^2}{\left(1-|\Gamma_{S\mathrm{DUT}i}|^2\right)|S_{21,\mathrm{DUT}}|^2} - \frac{T_C}{T_0}+1 \quad (4)$$

where P_{Ci} is the measured noise power for the ith source reflection coefficient $\Gamma_{S\mathrm{DUT}i}$ and Γ_{SRCVi} is the reflection coefficient of the network connected to the input of the receiver. With well-known Friis formula [19] for cascaded two-port, the DUT's noise figure can be calculated using

$$F_{\mathrm{DUT}i} = F_{\mathrm{TOT}i} - \frac{F_{RCVi}-1}{G_{\mathrm{DUT}i}} \quad (5)$$

where F_{RCVi} is the noise factor of the receiver calculated from the receiver's noise parameters for each source reflection coefficient and $G_{\mathrm{DUT}i}$ is the available gain of the DUT. Noise parameters of the DUT are determined using the same extraction procedure as with the receivers noise parameters.

V. Measurement Results

The operation of the measurement system was verified by measuring noise parameters of both passive and active on-wafer devices. Nine different source reflection-coefficient values were used during these measurements. The reflection-coefficient values used were distributed uniformly over the Smith chart. Minimum noise figure and normalized noise resistance of the receiver are shown in Figs. 5 and 6. The optimum source reflection coefficient was close to zero. The minimum noise figure shows uniform operation of the receiver over the entire 50–75-GHz band. With normalized noise resistance curve, there is a step in the curve after 66 GHz. Although the step remained in the results also after recalibration, this is suspected to be a fault. For a passive device, noise parameters can be calculated from measured S-parameters [20]–[22]. Comparison between the noise parameters determined using the developed measurement system and the values calculated from S-parameter measurements for passive device are shown in Figs. 7 and 8. The passive test item was nominally 40-Ω resistor connected in series between the probes. The resistor was measured from an old test wafer, where component characteristics differed from nominal values significantly. The resistor was selected because its S-parameters indicated a wide range for minimum noise figure. A good agreement between the measured and calculated data can be seen. There are only two significant deviations from calculated values in Fig. 8 at 73 and 74 GHz. Single origin for these errors can not be pointed out. Typical results obtained for an indium phosphide (InP) high electron-mobility transistor (HEMT) are shown in Figs. 9–12. Gate length and gatewidth of the HEMT device are 0.18 μm and 2 $\times$ 40 μm, respectively, and it was manufactured by DaimlerChrysler, Ulm, Germany. Drain voltage of 1.0 V and

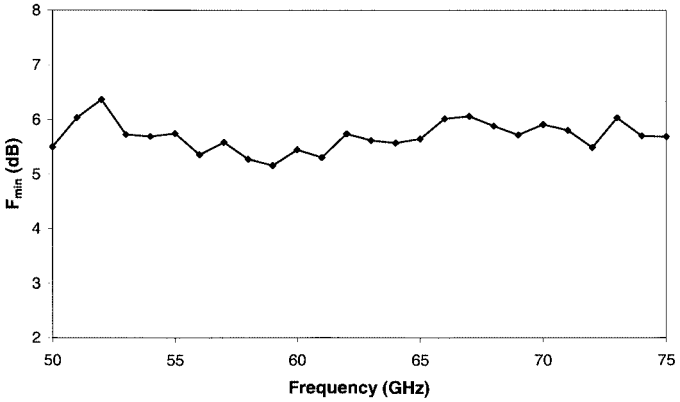

Fig. 5. Minimum noise figure of the receiver.

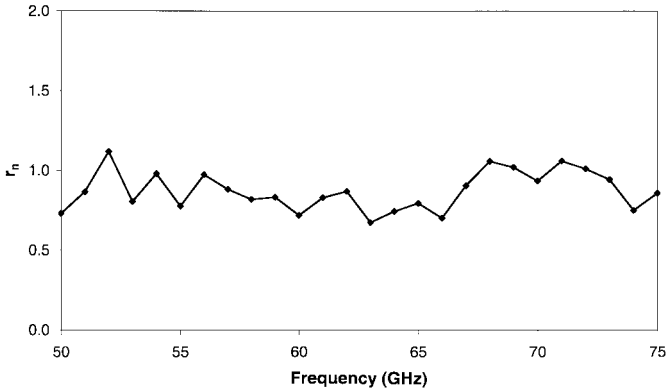

Fig. 6. Normalized noise resistance of the receiver.

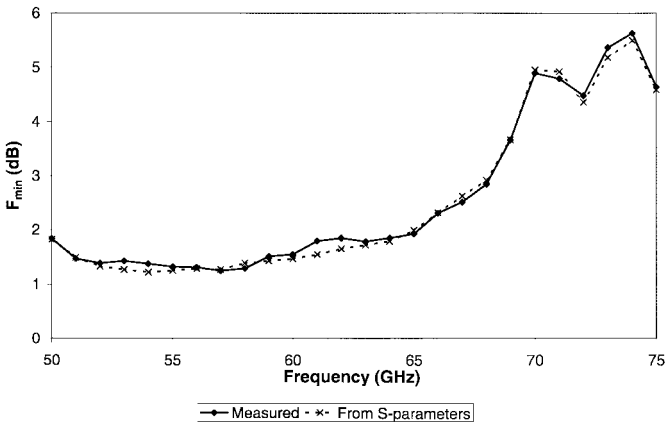

Fig. 7. Comparison of minimum noise figure between values measured using a wide-band measurement system and the value calculated from measured S-parameters for the passive on-wafer device.

drain current of 10 mA were used in the measurements. Values above 65 GHz have excess errors due to difficulties in the noise receiver calibration. Clear errors can be seen at the 66–68-GHz band, where the values of the minimum noise figure and noise resistance differ noticeably from the trend of preceding values. Similar behavior was seen on the normalized noise resistance of the receiver. The effect of the receiver noise resistance is greater with the HEMT device than with the resistor because receiver source reflection coefficient is further away from the center of the Smith chart with the HEMT device. Thus, the effect of some terms in (1) increases. These kinds of errors

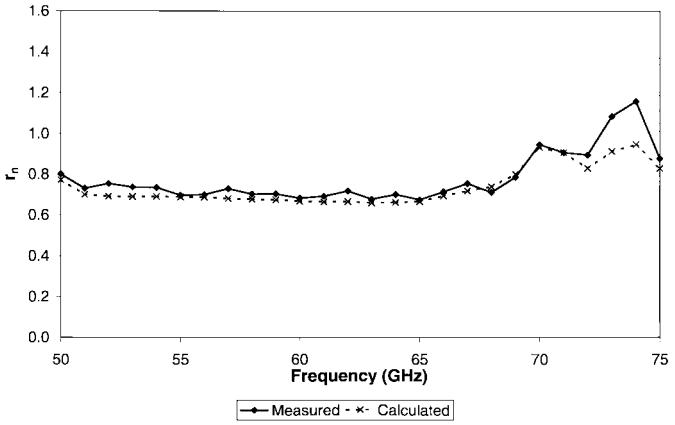

Fig. 8. Comparison of normalized noise resistance between values measured using a wide-band measurement system and the value calculated from measured S-parameters for the passive on-wafer device.

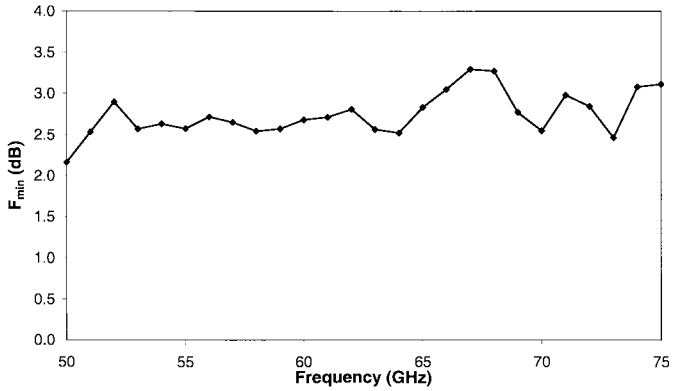

Fig. 9. Minimum noise figure measured for the InP HEMT device.

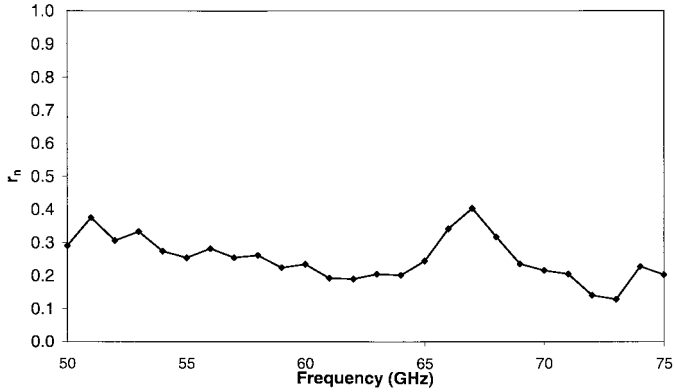

Fig. 10. Normalized noise resistance measured for the InP HEMT device.

can be clearly seen from the wide-band data, but may remain undiscovered when single-frequency measurements are done.

VI. Error Analysis

Almost 40 measured quantities affect the final values of the noise parameters. These include S-parameters, reflection coefficients, power measurements, ENR calibration of the noise source, and room temperature. To get an estimation of measurement accuracy, a Monte Carlo analysis [23] was carried out. In the analysis, random errors are added to the initial measured values and the noise parameters are calculated, e.g., 1000 times.

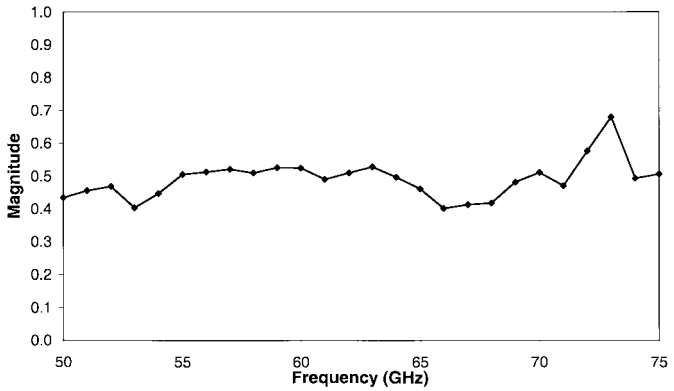

Fig. 11. Magnitude of optimum source reflection coefficient measured for the InP HEMT device.

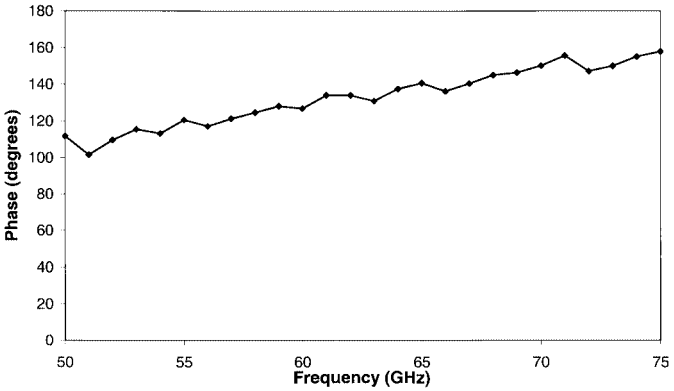

Fig. 12. Phase of optimum source reflection coefficient measured for the InP HEMT device.

TABLE I
Uncertainties for Measured Parameters

Parameter	Standard uncertainty	Uncertainty type
$S_{11,TUN}$, $S_{22,TUN}$	0.005	A, B
$S_{12,TUN}$, $S_{21,TUN}$	0.006	A, B
$S_{11,PRB}$, $S_{22,PRB}$	0.036	B
$S_{12,PRB}$, $S_{21,PRB}$	0.005	B
$S_{11,DUT}$, $S_{22,DUT}$	0.036	B
$S_{12,DUT}$, $S_{21,DUT}$	0.05	B
Γ_{LRCV}	0.036	B
Γ_{SDUT}	0.036	A, B
Γ_{NS}	0.005	B
ENR (dB)	0.06	B
P_H, P_C (dB)	0.04	B
T_C (K)	0.82	B

Statistical analysis is then performed to the obtained noise-parameter sets. To get values for random error distributions, uncertainties were divided into A- and B-type uncertainties, as suggested in [24]. A-type uncertainties are determined through statistical analysis and B-type uncertainties by any other means (i.e., from literature). Prior work with manual on-wafer measurement system provided most of the information [25]. Uncertainties used in the error analysis are listed in Table I. Rectangular distribution was used for S-parameter, reflection coefficient, and power measurement errors. Triangular distribution was used for ambient temperature. Deviations of the minimum noise figure and the optimum source reflection coeffi-

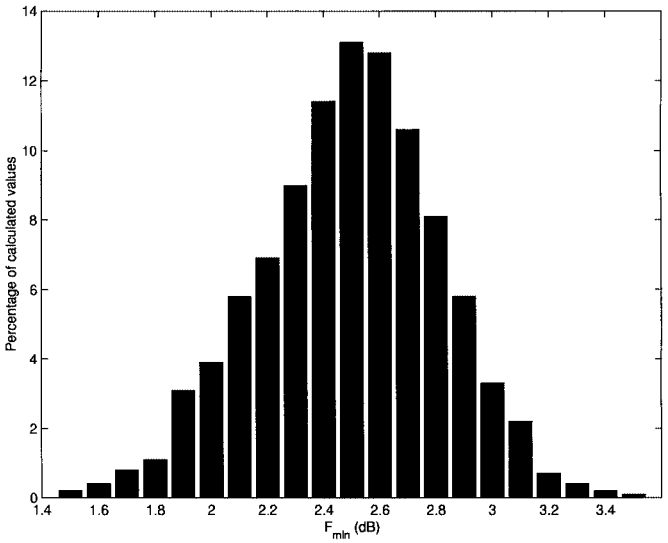

Fig. 13. Deviation of the minimum noise figure obtained in the Monte Carlo analysis with 1000 runs at 57 GHz.

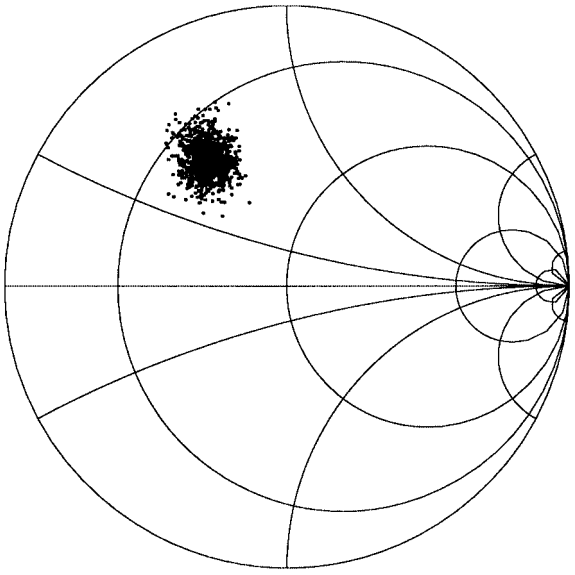

Fig. 14. Scattering of the optimum source reflection coefficient obtained in the Monte Carlo analysis with 1000 runs at 57 GHz.

TABLE II
MEASURED NOISE PARAMETERS AND CORRESPONDING CONFIDENCE BOUNDARIES FOR THE HEMT DEVICE AT 57 GHz

Parameter	F_{min}	r_n	$\lvert\Gamma_{opt}\rvert$	$\angle\Gamma_{opt}$
Measured value	2.65 dB	0.25	0.57	121°
2σ (95.5 %) confidence boundary	± 0.6 dB	± 0.06	± 0.1	± 9°

cient are presented in Figs. 13 and 14. S-parameters of the DUT and source reflection-coefficient measurement $(\Gamma_{S\mathrm{DUT}})$ were found to be the main sources of errors. Confidence boundaries depend heavily on the test device. For example, the noise paraboloid defined by (1) for an HEMT device has a very flat bottom due to a low value of r_n. Thus, even a major displacement of the optimum source reflection coefficient has only a little effect on the shape of the noise paraboloid. This leads to a wide confidence boundary for the optimum reflection coefficient. As an example, the measured values for the HEMT device at 57 GHz with the corresponding 2σ confidence boundaries are given in Table II. Obtained boundaries correspond to observed ripple well when clearly erroneous values are discarded.

VII. CONCLUSIONS

A unique wide-band automated on-wafer noise parameter measurement setup has been built and its performance has been demonstrated by measuring noise parameters for both passive and active on-wafer devices. Wide-band noise-parameter measurements at millimeter-wave frequencies are important for accurate interpretation of the measured results. For example, if measurements had been made on a single frequency at 67 GHz, false results would have been obtained due to problems with the noise receiver calibration. These kinds of frequency-dependent systematic errors can be revealed only when wide-band measurements are performed. The wide-band on-wafer measurement system will also be an important tool in development and verification of device models, as well as in device characterization.

ACKNOWLEDGMENT

The authors would like to thank P. Kangaslahti, P. Jukkala, and N. Hughes, all of Ylinen Electronics Ltd., Kauniainen, Finland, for lending us the wide-band LNA. The authors would also like to recognize the invaluable support and comments of T. Närhi, European Space Agency (ESA), Noordwijk, The Netherlands, as well as T. Karttaavi, J. Varis, and H. Hakojärvi, all of the Millimeter Wave Laboratory of Finland–MilliLab, VTT TECHNICAL RESEARCH CENTRE OF FINLAND, Espoo, Finland.

REFERENCES

[1] J. Laskar, M. R. Murti, S. Y. Yoo, E. Gebera, and H. M. Harris, "Development of complete on-wafer cryogenic characterization: S-parameters, noise parameters and load-pull," in *Eur. GaAs and Related III–V Compounds, Application Symp. Dig.*, Amsterdam, The Netherlands, 1998, pp. 33–38.

[2] M. Lahdes, J. Tuovinen, and M. Sipilä, "60 GHz on-wafer noise measurements using cold-source method," in *49th ARFTG Conf. Dig.*, 1997, pp. 146–154.

[3] M. Lahdes and J. Tuovinen, "V-band on-wafer noise parameter measurements," in *Proc. GAAS*, 1998, pp. 39–44.

[4] J. Tuovinen, M. Lahdes, T. Karttaavi, and H. Hakojärvi, "Millimeter wave on-wafer testing at room and cryogenic temperatures," in *Proc. 7th Int. Recent Advances in Microwave Technology Symp.*, 1999, pp. 415–418.

[5] M. Kantanen, M. Lahdes, J. Tuovinen, T. Vähä-Heikkilä, P. Kangaslahti, P. Jukkala, and N. Hughes, "A wideband automated measurement system for on-wafer noise parameter measurements at 50–75 GHz," in *Proc. GAAS*, 2001, pp. 255–258.

[6] T. A. Alam, R. D. Polard, and C. M. Snowden, "The determination of on-wafer noise parameters in W-band," in *Proc. 27th Eur. Microwave Conf.*, 1997, pp. 687–691.

[7] H. Rothe and W. Dahlke, "Theory of noisy four poles," in *Proc. IRE*, vol. 44, 1956, pp. 811–818.

[8] V. Adamian and A. Uhlir, "A novel procedure for receiver noise characterization," *IEEE Trans. Instrum. Meas.*, vol. IM-22, pp. 181–182, June 1973.

[9] R. Meierer and C. Tsironis, "An on-wafer noise parameter measurement technique with automatic receiver calibration," *Microwave J.*, vol. 38, pp. 22–37, 1995.

[10] J. Tuovinen, P. Kangaslahti, P. Haapanen, N. Hughes, P. Jukkala, T. Karttaavi, O. Koistinen, M. Lahdes, H. Salminen, J. Tanskanen, and S. Urpo, "Development of 70 GHz receivers for the Planck LFI," *Astrophys. Lett. Commun.*, vol. 37, pp. 181–187, 2000.
[11] A. Davidson, K. Jones, and E. Strid, "LRM and LRRM calibrations with automatic determination of load inductance," in *36th ARFTG Conf. Dig.*, 1990, pp. 57–62.
[12] G. F. Engen and C. A. Hoer, "Thru-reflect-line: An improved technique for calibrating the dual six port automatic network analyzer," *IEEE Trans. Microwave Theory Tech.*, vol. 27, pp. 987–993, Dec. 1979.
[13] R. T. Webster, A. J. Slobodnik, and G. A. Roberts, "Determination of InP HEMT noise parameters and S-parameters to 60 GHz," *IEEE Trans. Microwave Theory Tech.*, vol. 43, pp. 1216–1225, June 1995.
[14] R. P. Meys, "A triple-through method for characterizing test fixtures," *IEEE Trans. Microwave Theory Tech.*, vol. 36, pp. 1043–1046, June 1988.
[15] C. L. Hammond and K. L. Virga, "Network analyzer calibration methods for high-density packaging characterization and validation of simulation methods," in *Proc. Electronic Components and Technology Conf.*, 2000, pp. 519–525.
[16] M. Nishimoto, M. Hamai, J. Laskar, and R. Lai, "On-wafer calibration techniques and applications at V-band," *IEEE Trans. Microwave Guided Wave Lett.*, vol. 4, pp. 370–372, Nov. 1994.
[17] G. I. Vasilescu, G. Alquie, and M. Krim, "Exact computation of two-port noise parameters," *Electron. Lett.*, vol. 25, pp. 292–293, 1989.
[18] L. Escotte, R. Plana, and J. Graffeuil, "Evaluation of noise parameter extraction methods," *IEEE Trans. Microwave Theory Tech.*, vol. 41, pp. 382–387, Mar. 1993.
[19] H. T. Friis, "Noise figure of radio receivers," in *Proc. IRE*, vol. 32, July 1944, pp. 419–422.
[20] A. Fraser, E. Strid, B. Leake, and T. Burcham, "Repeatability and verification of on-wafer noise parameter measurements," *Microwave J.*, vol. 31, no. 11, pp. 172–176, Nov. 1988.
[21] A. Boudiaf, C. Dubon-Chevallier, and D. Pasquet, "Verification of on-wafer noise parameter measurements," *IEEE Trans. Instrum. Meas.*, vol. 44, pp. 332–335, June–July 1995.
[22] E. Strid, "Noise measurements for low-noise GaAs FET amplifiers," *Microwave Syst. News*, vol. 10, pp. 62–70, 1981.
[23] W. H. Press, B. P. Flannery, S. A. Teukolsky, and W. T. Vetterling, *Numerical Recipes, The Art of Scientific Computing*. Cambridge, MA: Cambridge Univ. Press, 1986.
[24] B. N. Taylor and C. E. Kuyatt, "Guidelines for evaluating and expressing the uncertainty of NIST measurement results," NIST, Boulder, CO, Tech. Note 1297, 1994.
[25] M. Lahdes, "Uncertainty analysis of V-band on-wafer noise parameter measurement system," in *Proc. 28th Eur. Microwave Conf.*, 1998, pp. 445–450.

Mikko Kantanen received the Master of Science degree in electrical engineering degree from the Helsinki University of Technology (HUT), Espoo, Finland, in 2001.

Since 1999, he has been with the Millimeter Wave Laboratory of Finland–MilliLab, VTT TECHNICAL RESEARCH CENTRE OF FINLAND, Espoo, Finland, initially as a Trainee Research Scientist and, since 2001, as a Research Scientist involved with noise measurements at millimeter waves. He is currently also involved with other millimeter-wave activities including on-wafer measurement systems, monolithic microwave integrated circuit (MMIC) design, and passive imaging.

Manu Lahdes received the Master of Science degree in electrical engineering degree from the Helsinki University of Technology, Espoo, Finland, in 1996.

Since 1996, he has been with a Research Scientist the Millimeter Wave Laboratory of Finland–MilliLab, VTT TECHNICAL RESEARCH CENTRE OF FINLAND, Espoo, Finland. His research interests in the millimeter-wave area have been on-wafer noise parameter measurements, cryogenic on-wafer measurements, active device modeling, and MMIC design and testing. He has authored or coauthored several papers. His current activities also include passive millimeter imaging.

Tauno Vähä-Heikkilä (S'01) received the B.S. and M.S. degrees in physics from the University of Turku, Turku, Finland, in 2000 and 2001, respectively. His M.S. thesis concerned W-band on-wafer noise-parameter measurements.

He was a Trainee Research Scientist and, since 2002, he has been a Research Scientist with the Millimeter Wave Laboratory of Finland–MilliLab, VTT TECHNICAL RESEARCH CENTRE OF FINLAND, Espoo, Finland. He is also currently a Visiting Scholar with the Radiation Laboratory, The University of Michigan at Ann Arbor. His research interests include RF microelectromechanical systems (MEMS) and millimeter-wave on-wafer measurements.

Mr. Vähä-Heikkilä has been a secretary for the IEEE Antennas and Propagation (AP)/Electron Devices (ED)/Microwave Theory and Techniques (MTT) Finland Chapter since 2001.

Jussi Tuovinen (S'86–M'91) received the Dipl.Eng., Lic.Tech., and Dr.Tech. degrees in electrical engineering from the Helsinki University of Technology (HUT), Espoo, Finland, in 1986, 1989, and 1991, respectively.

From 1986 to 1991, he was a Research Engineer with the HUT Radio Laboratory, where he was involved with millimeter-wave antenna testing for the European Space Agency (ESA), quasi-optical measurements, and Gaussian beam theory. From 1991 to 1994, he was a Senior Post-Doctoral Fellow with the Five College Radio Astronomy Observatory, University of Massachusetts, Amherst, where he studied holographic testing methods and developed frequency multipliers up to 1 THz. From 1994 to 1995, he was a Project Manager with the HUT Radio Laboratory, where he was involved with hologram compact antenna test range (CATR) and 119-GHz receiver development for Odin-satellite. He is currently a co-investigator and heads development of 70-GHz receivers for the low-frequency instrument of the ESA Planck Surveyor. His research activities also includes development of methods for on-wafer testing of integrated circuits and components. He is currently a Research Professor with VTT TECHNICAL RESEARCH CENTRE OF FINLAND Information Technology and a Director of the Millimeter Wave Laboratory of Finland–MilliLab, ESA External Laboratory. From 2001 to 2002, he was a Visiting Researcher with the University of Hawaii at Manoa, where he developed communications methods using retrodirective antennas. He has authored or coauthored over 100 papers.

Dr. Tuovinen is a past secretary of the Finnish National Committee of the Committee on Space Research (COSPAR) and the IEEE Finland Section. He was also the executive secretary of the Local Organizing Committee of the 27th Plenary Meeting of COSPAR, held in 1988. In 1998, he was a co-chairman of the Second ESA Workshop on Millimeter Wave Technology and Applications. He has served as a chairman of the IEEE Microwave Theory and Techniques (MTT)/Antennas and Propagation (AP) Finland Chapter. He is the chairman of the Third ESA Workshop on Millimeter Wave Technology and Applications. He was the recipient of an ESA Fellowship for multiplier work at the University of Massachusetts in 1992 and again in 1993.